Journal of New Technology and Materials
(JNTM)
J. New Technol. Mater.
Vol. 11, N°02 (2021)23-28

OEB Univ. Publish. Co.

Mixed surfactant system SANS spectrum modelisation

H. Belarbi [a,b *] and F. Bouanani [a,c]

[a] *Laboratory of Macromolecular Physical Chemistry, Faculty of Exacts and Applied Sciences, University of Oran 1 Ahmed Ben Bella, El Mnaouer BP 1524, Oran, Algeria.*

[b] *Department of Basic Teachings in Sciences and Technologies (EBST), Faculty of Technology, Djillali Liabes University, Ben MHidi BP 89, Sidi Bel Abbes, Algeria.*

[c] *Department of engineering process, National polytechnic school Maurice Audin(ENPO), El Mnaouer BP 1523, Oran, Algeria*

*Corresponding author, email: b_hayet24@yahoo.fr

Selected paper of JMSM-2020, received date: Aug. 02, 2021 ; accepted date: Sep. 30, 2021

Abstract

In this work, small angle neutrons scattering (SANS) was exploited to investigate the inner structure of a mixed system containing a nonionic fluorosurfactant (undecafluoro-n-pentyl-decaoxyethylene ether ($C_5F_{11}(EO)_{10}$; FSO100) and 66% of a cationic surfactant dodecyltrimethyl ammonium bromide (DTAB) on a wide range of spatial resolution, at 25 °C . The data analysis of the corrected and normalized scattered intensities was based on the coexistence of two micellar populations, namely, homogeneous polydisperse spheres and stacked core–shell *disc-like micelles. This fitting model was used assuming either a mixed micellization or a F/H segregation phenomena. The obtained results support to some degree the micellar mixing but do not exclude completely the occurrence of an intra- or extra-micellar segregation.* A predictive stacking parameter calculated for the mixed system indicates a morphologic transformation with regards to the pure surfactants.

Keywords: FSO-100/DTAB; SANS; mixed micelle; fluorinated nonionic surfactant; cationic surfactant; bimodal distribution.

1. Introduction

Mixtures of surfactants have been subject of a great deal of interest [1,2] because of their various applications in many fields such in enhanced oil recovery [3], extraction of organic pollutants [4, 5] and stabilization of nanoemulsions [6]. In particular, the fluorinated/hydrogenated mixtures have been successfully used in many industrial areas such as firefighting [7], detergency [8] and recently in preparation of mesoporous materials [9] and gold nanoparticules [10]. Indeed, adding a small amount of a fluorinated surfactant to an hydrogenated one improves some micellar and surface properties, in particular in the reduction of the critical micellar concentration (cmc) [11]. This effect is mainly due to the very pronounced hydrophobic as well as oleophobic character of the fluorinated compounds [12]. Indeed, they have remarkable and unique surface properties, in particular the ability to reduce dramatically the surface tension [13]. This improvement in the physicochemical properties of the fluorine/hydrogen (F/H) mixed systems is generally related to the synergism between the hydrogenated and fluorinated molecules, depending on the characteristics of both components. Moreover, the fluorinated chain is also stickier and bulkier than its hydrocarbon homologue [14-16]. So, this type of mixtures self-assemble in aqueous media yielding a variety of micellar structures such as spherical, ellipsoidal, cylindrical, wormlike and threadlike [17-19].

On the other hand, hydrocarbon/fluorocarbon assemblies are still the subject of controversy regarding the structure of the formed micelles, due to the competition between head-groups electrostatic interactions favouring the mixing and the lipophobicity of fluorinated chains promoting segregation [20]. Indeed, if some works [21] seem to indicate the existence of a F/H segregation either intra- or inter-micellar [22-24], with the formation of extended separated domains, other studies[25-27] claimed the emergence of mixed homogeneous micelles [28,29].

More recently [30], it appeared that the features of F/H assemblies are closely associated to the mutual surfactant interactions nature. Mixing could possibly be obtained in micellar aggregates when a strong electrostatic interaction between the fluorinated and hydrogenated head-groups overcome the mutual phobicity (antagonism) of the chains.

In an attempt to contribute clarify these apparent disagreements in the literature, several investigation methods including different spectroscopic techniques such as fluorescence, 1H and 19F NMR [31] and small angle neutron scattering (SANS) [32, 33], as well as the analysis of experimental tensiometric data using thermodynamic mixed micellization models, have been used [34]. SANS [35, 36] appears as the most powerful tool to elucidate the inner structure of the micelles. Its choice as the main method of investigation is motivated by its high spatial resolution besides its capacity to study the mixed surfactant systems in their native states since micellar interactions in

concentrated media may be generally straight forwardly taken into account.

The aim of the present work is to study the mixed micellization of a well known cationic compound dodecyltrimethylammonium bromide (DTAB) [37] with a nonionic fluorinated one, n-undecafluoro n-pentyldecaoxyethylene ether (C5F11EO10) [38] with a molecular proportion of 66% DTAB. It should be noted that the particularity of this compound is that it is composed of ethylene oxide units directly linked to a perfluoroalkyl chain. Our interest in this surfactant is based on the fact that, to our knowledge, it remains poorly studied [34, 39] despite its various interesting applications [40]. This mixed surfactant system was previously characterized physico-chemically for different proportions of DTAB [38]. Here, the structure of this particular mixture is examined using SANS with regards to the micellar particle mean size and size distribution

2. Experimental

2.1. Materials

The nonionic fluorinated surfactant, C5F11EO10, was provided by Zonyl as the FSO100 brand having a purity of 98%. The cationic one, DTAB (C12H25N+(CH3)3,Br-), was supplied by Sigma Aldrich with a purity of 98%. Both were used without further purification. The solvent is deuterated water for SANS measurements.

2.2. Small angle neutron scattering

The data acquisition was performed on the spectrometer PAXE of the Léon Brillouin Laboratory at Saclay in three different setups in order to cover a large domain of momentum transfer. Despite a convenient transmission (around 0.7), the very high-scattered intensity at very small scattering angles generated a small but significant saturation of the electronics which was not corrected during the experiment. Thus, the corresponding data were not taken into account in the data fitting process. The raw data were corrected for sample transmission, solvent and empty cell contributions and detector efficiency by a standard procedure, then normalized and converted into an absolute scale of the scattered intensity.

2.3. Theory /Calculation

2.3.1 SANS Theory

SANS experiments consist in measuring the static neutron intensity scattered at small angles. The scattering pattern from a given sample can be described in terms of the Fourier transform of the correlations of the scattering length density distribution [41]. In the case of a system made of homogeneous polydisperse spheres [42] dispersed in a solvent, the isotropic coherent scattered intensity is given by the following equation:

$$I(Q) = \frac{N}{V}\left(\left\langle |F(Q)|^2 \right\rangle - \left|\langle F(Q)\rangle\right|^2\right) + \frac{N}{V} P(Q)S(Q) \qquad (1)$$

Here N is the number of particles per unit volume of the sample and Q is the magnitude of the scattering vector which is related to the incident radiation wavelength λ and the scattering angle θ, by:

$$Q = \frac{4\pi}{\lambda}\sin\frac{\theta}{2} \qquad (2)$$

S(Q) is the particle structure factor which takes into account the inter-particle interactions and F(Q) is the particle diffusion function or form factor.

-In the case of spherical particles it is usual to define P(Q) as:

$$P(Q) = \left|\langle F(Q)\rangle\right|^2 = \int_0^\infty V^2(\rho - \rho_s)^2 \left| f(Q,R)\right|^2 \cdot h(R)dR \qquad (3)$$

$$f(Q,R) = V^2 \Delta\rho \left[3\frac{\sin(QR) - qR\cos(QR)}{(QR)^3}\right]^2 \qquad (4)$$

In this expression, ρ and ρ_s are the scattering length densities of the homogeneous particle and the solvent, respectively. *f*(Q,R) is the first order spherical Bessel function. *h*(R) is the radii distribution which is generally taken as the Schulz–Zimm function [43]. It is characterized by the mean particle radius $\overline{R}$ and the width of the distribution which is related to the size polydispersity factor P.

The contribution of S(Q), associated to the correlations between the particle spatial positions, is estimated to a first approximation on the basis of the excluded volume model [44] where the particle size is taken as $\overline{R}$. In our case the volume fraction occupied by the particles is equal to φ=0,006.

-In the case of stacked disks particles [45], the total coherent scattered intensity can be calculated assuming that the next neighbor distance (d-spacing) in a stack of parallel discs obeys a Gaussian distribution. The expression of I(Q) is then given by:

$$I(Q) = N\int_0^{\pi/2} [\Delta\rho_t (V_t f_t(Q) - V_c f_c(Q)) + \Delta\rho_c V_c f_c(Q)]^2 S(Q)\sin\varphi d\varphi \qquad (5)$$

where N is the number of discs per unit volume and $\Delta\rho_i = \rho_i - \rho_{solvent}$ represents the corresponding contrast of species i with respect to the solvent. t and c indicated total and core of single disk, φ is the angle between $\vec{Q}$ and the axis of the disc.

V_t and V_c are the total and core volumes of a single disc, respectively. R, d, and 2h are the radius of the disc, the thickness of the layer and the core thickness, respectively. f_t (Q) and f_c (Q) are the scattering functions of the layer and core, respectively:

$$\left\langle f_t^2(Q)\right\rangle_\varphi = \int_0^{\pi/2}\left[\left(\frac{\sin(Q(d+h))\cos\varphi}{Q(d+h)\cos\varphi}\right)\left(\frac{2J_1(QR)\sin\varphi}{QR\sin\varphi}\right)\right]^2 \sin\varphi d\varphi \quad (6)$$

$$\left\langle f_c^2(Q)\right\rangle_\varphi = \int_0^{\pi/2}\left[\left(\frac{\sin(Qh)\cos\varphi}{Qh\cos\varphi}\right)\left(\frac{2J_1(QR)\sin\varphi}{QR\sin\varphi}\right)\right]^2 \sin\varphi d\varphi \quad (7)$$

where J_1 is the first Bessel function and S(Q) is the structure factor as proposed by Kratky and Porod [46].

2.3.2 Predictive calculations (packing parameter p):

According to Israelachvili et al. [47], the arrangement of surfactant molecules in a micelle is mainly determined by molecular geometrical factors whose expression is manifested through a stacking parameter p. In the case of a surfactant mixture, the expression of p takes the following form [48]:

$$p = \frac{(\sum_i V_i X_i^m)}{(\sum_i a_i X_i^m)\ (\sum_i l_i X_i^m)} \quad (8)$$

a_i being the corresponding polar head area and X_i^m is the composition of surfactant i in a micelle.
V_i and l_i are the volume of exclusion per monomer of each species i in the aggregate and the maximum chain length of the hydrophobic chain of surfactant i, respectively. These parameters are given by the following equations for the hydrogenated surfactant [49]:

$$V_i\ (nm^3) = 0.0274 + 0{,}0269\ n_c \quad (9)$$

$$l_i\ (nm) = 0.154 + 0.127\ n_c \quad (10)$$

while for the fluorinated component [50] one has:

$$V_i\ (nm^3) = 0.0545 + 0{,}0380\ n_c \quad (11)$$

$$l_i\ (nm) = 0.200 + 0.134\ n_c \quad (12)$$

where n_c is the number of carbon atoms of the chain.

3. Results

3.1. Prediction shape:

The mixture stacking parameter value is deduced from equation (8) assuming either an ideal (Clint model) [51], or a regular behavior using the Rubingh analysis [52]. In the first case, the value of p equals 0.68, suggesting the preferential formation of vesicles or bilayer micelles. This result is similar to that obtained for pure FSO100 for which p=0.69 [39] However, using Rubingh model, an increase of p value (0.71) is observed knowing that p corresponding to pure DTAB (0.33) [53] is in favor of a spherical form [53, 54]. Hence, adding 34% of FSO100 should lead to the formation of bilayer or lamellar structures in the mixture. Accordingly, the mixed micelles would suffer a transformation correlated with the increase in the curvature radius as the proportion of FSO100 rises in the medium. A comparable predictive result was observed by H. Otmani et al. [39] for FSO100/DeTAB (decyltrimethylammonium bromide) mixed system and justified in a similar way.

3.2 SANS results:

The absolute scale of mixed DTAB/FSO100 SANS spectrum corrected for the flat incoherent background, as deduced from the highest Q values, and normalized, with respect to the flat incoherent scattering of water, is presented in fig. 1. The scattered intensity shows two decreasing functions of Q, separated by a Q^0 dependence in the intermediate domain [55], with a monotonous $Q^{-1.8}$ dependence at the lowest Q values. This latter dependence close to Q^{-2} is generally related to the diffusion of a planar particle [56], whereas the spectrum slope marked change indicates probably the presence of two micellar populations. At high Q values, the scattered intensity behavior suggests the presence of a micellar size around 10 Å, while at small Q values another micellar dimension (in the 10^3 Å range) is expected.
Taking into account the presence of two kinds of micelles, the fitting model represents the sum of two contributions. While the first is due to homogeneous polydisperse spheres as shown on fig. 2-a, the second is correlated to stacked disks as can be seen on fig. 2-b. The coexistence of these two kinds of micelles may occur either as mixed micellization takes place or through a segregation phenomena.
The above assumptions are made taking into account the possible well-known self-sorting of fluorinated surfactants [57] or the possibility of some mixing of H/F surfactants within mixed micelles [58]. The latter mechanism is possible when the hydrogenated and the fluorinated surfactants have either the same or opposite charges,

inducing strong interactions between head-groups, as seen in the introduction

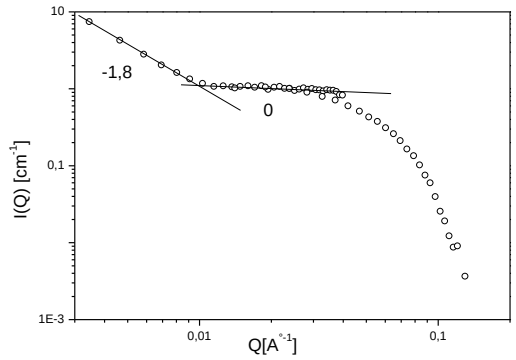

Figure 1. SANS spectrum on logarithmic scales with linear fits.

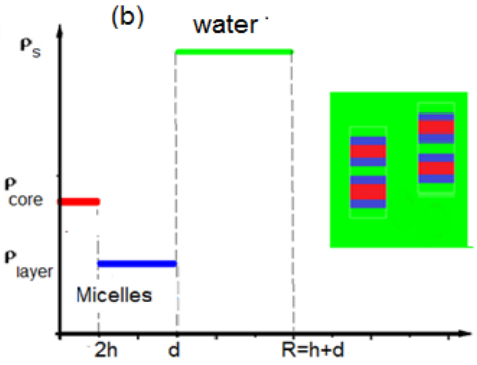

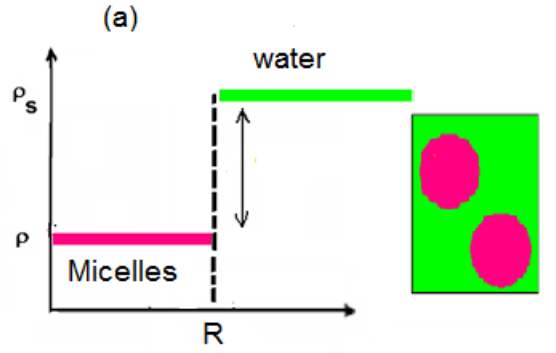

Figure 2. Scattering length density profile of: (a) the homogeneous polydisperse spheres and (b) stacked disks models.

Fig. 3 represents the mixed (FSO100/DTAB) SANS spectrum best fit corresponding to a bimodal system characterized by the coexistence of polydisperse homogeneous spherical particles and stacked core-shell disks assemblies. If assuming, first, a micellar segregation ($X^{m}_{DTAB} = 0$) then the best fit is obtained for a large proportion of spherical micelles ($\overline{R}_{Sphere}$ =34 Å and p = 0.15) linked to a stronger contribution in the scattered intensity at high Q. Whereas, the co-existing stacked disks micellar population (10%, $\overline{R}_{Disk}$ =76000 Å, 2h = 17 Å, d = 26 Å and p=0.15) shows a stronger contribution in the scattered intensity at small Q. The highest partial volume fraction of the spherical micelles (ϕ_1) that could be incorporated in the model system without changing significantly the goodness of this fit, as it can be seen from fig. 3, is about 90% of the total micellar volume fraction.

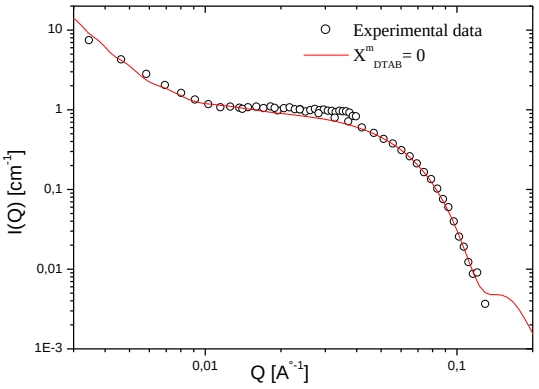

Figure 3. SANS spectrum best fit (full line) corresponding to the sum of two model populations: polydisperse homogeneous spheres (ϕ_1 = 90%, $\overline{R}_{Sphere}$ =34 Å and p = 0.15) and stacked disks (ϕ_2=10%, 2h = 17 Å, d = 26 Å, $\overline{R}_{Disk}$ =76000 Å and p = 0.15).

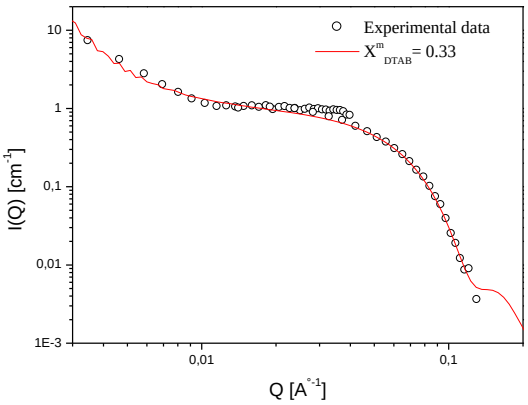

Figure 4. SANS spectrum best fit (full line) corresponding to the sum of two models populations: polydisperse homogeneous spheres (ϕ_1=50%, $\overline{R}_{Sphere}$ =34 Å and p = 0.15) and stacked disks (ϕ_2=50% , 2h = 36 Å, d = 16 Å, $\overline{R}_{Disk}$ = 6000 Å and p =0.15).

If the mixed micellisation of FSO100 and DTAB occurs, as a second hypothesis, the micellar composition can then be deduced from Rubingh's analysis [38] which leads to $X_{DTAB}^{m} = 0.33$. Thus, the best fit taking into account the coexistence of two populations provides the following results reported on fig. 4:

- polydisperse homogeneous spherical micelles,

$\overline{R}_{Sphere}$ =34 Å, p = 0.15;

- stacked core–shell disks,

$\overline{R}_{Disk}$ = 6000 Å, 2h= 36 Å, d=16 Å, p= 0.15.

In this model, the partial volume fraction of the spherical micelles (ϕ_i) contribution is only 50%.

4. Conclusion

From the data analysis, it appears that the mixed hydrogenated/fluorinated system studied presents a very broad particle size distribution, probably characterized by a bimodal feature. This is attributed to the presence of two kinds of micelles (spherical and staked disks) coexisting in the solution above the cmc. The flat morphology was predicted according to the packing parameter of the mixed system.

If a demixing occurs, the average radius of the spheres population is 34Å, whereas the size of the stacked disks is about 76000 Å. In this case, the proportion of the spherical micelles seems to represent the predominant species of the total solubilized matter. However, if assuming mixed micellisation, the contribution of the spherical micelles is about 50% and its mean size is about 34 Å.

Thus, these results support to some degree the micellar mixing hypothesis but do not exclude completely the possible occurrence of an intra- or extra-micellar segregation. A much more comprehensive study using for instance several neutron contrasts and combining different investigation methods are required to characterize this system in detail.

Acknowledgments

The authors thank Prof. Dalila Bendedouch for providing invaluable guidance throughout this research, and Pr José Teixeira for access to Saclay instruments (Léon Brillouin laboratory, CEA, french)

References

[1] J. F. Scamehorn, In Phenomena in Mixed Surfactant Systems Ed.,J F Scamehorn, ACS Symposium Series, Vol 311, American Chemical Society, Washington DC, 1989.

[2] P.M. Holland, D.N. Rubingh, Mixed Surfactant Systems., An Overview, ACS Symposium Series, Vol. 501, American Chemical Society, Washington DC, 1992.

[3] R. Kumari, A. Kakati, R. Nagarajan, and J.S. Sangwai, J. Disper. Sci. Tech. 40 (2019) 969.

[4] K. Jagajjanani Rao, S. Paria, J. Phy. Chem. B. 113 (2009) 474.

[5] T. Abram, R. Chfaira, J. Mater. Envir. Sci. 6 (2015) 491.

[6] T. Chuacharoen, S. Prasongsuk and C. M. Sabliov, Molecules. 24 (2019) 2744.

[7] A.V. Vinogradov, D.S. Kuprin, I.M. Abduragimov, G.N. Kuprin, E. Serebriyakov, V.V. Vinogradov, ACS Appl. Mater. Interf. 8 (2016) 294.

[8] J.L. Blin, N. Henzel, M.J. Stebe, J. Coll. Interf. Sci. 302 (2006) 643.

[9] K. Assaker, M. J. Stébé, J. L. Blin, Coll. Surf. A: Physicochem. Eng. Asp. 536 (2018) 242.

[10] M. Şologan, D. Marson, S. Polizzi, P. Pengo, S. Boccardo, S. Pricl, P. Posocco and L. Pasquato, ACS Nano. 10 (2016) 9316.

[11] J.M. Rosen, Phenomena in Mixed Surfactant Systems, ACS Symposium Series 311, Washington, 2004.

[12] R. Oda, I. Huc, D. Danino and Y. Talmon, Langmuir. 16 (2000) 9759.

[13] Q. Yin, W. Xue, Y. Bai, W. Wang, X. Ma, Z. Du and G. Wang, J. Ind. Eng. Chem. 42 (2016) 63.

[14] K. Szymczyk, J. Fluor. Chem. 150 (2013) 109.

[15] K.V. Schubert, E.W. Kaler, Coll. Surf. A: Physicochem. Eng. Asp. 84 (1994) 97.

[16] J. Skvarla, M. Uchman, K. Procházka, Z. Tošner, V. M. Garamus, S. Pispas and M. Štěpánek, Coll. Surf. A: Physicochem. Eng. Asp. 443 (2014) 209.

[17] Z. O. Et-Tarhouni, E. Carter, D. M. Murphy, P. C. Griffiths, O. T. Mansour, S. M. King and A. Paula, Coll. Surf. A: Physicochem. Eng. Asp. 492 (2016) 255.

[18] K. Morishima, S. Sugawara, T. Yoshimura and M. Shibayama, Langmuir. 33 (2017) 6084.

[19] N. Jiang, Y. Sheng, C. Li and S. Lu, J. Molecul. Liquids. 268 (2018) 249.

[20] N. Hassan, J.M. Ruso and A. Pineiro, Langmiur. 27 (2011) 9719.

[21] E. Frotscher, J. Höring, G. Durand, C. Vargas, and S. Keller, Anal. Chem. 89 (2017) 3245.

[22] V Peyre, Curr. Opini. Coll. Interf. Sci. 14 (2009) 305.

[23] M. Kadi, P. Hansson, M. Almgren and I. Furo, Langmuir. 18 (2002) 9243.

[24] S. L. Dong, G. Xu and H. Hoffmann, J. Phy. Chem. B. 112 (2008) 9371.

[25] V. Peyre, S. Patil, G. Durand and B. Pucci, Langmuir. 23 (2007)11465.

[26] L. Nordstierna, I. Furo and P. Stilbs, J. Am. Chem. Soc. 128 (2006) 6704.
[27] M. E. Amato, E. Caponetti, D. C. Martino and L. Pedone, J. Phy. Chem. B. 107(2003) 10048.
[28] T. Y. Nakano, G. Sugihara, T. Nakashima and S. C. Yu, Langmuir. 18 (2002) 8777.
[29] P. Barthelemy, V. Tomao, J. Selb, Y. Chaudier and B. Pucci, Langmuir. 18 (2002) 2557.
[30] M. Şologan, M. Boccalon, S. Bidoggia, C. Gentilini, L. Pasquato and P. Pengo, Supramol. Chem. 29 (2017) 808.
[31] S.L. Dong, X. Li, G.Y. Xu and H. Hoffmann, J. Phy. Chem. B. 111(2007) 5903.
[32] F. Bouanani, D. Bendedouch, J. Teixeira, L. Marx and P. Hemery, Coll. Surf. A: Physicochem. Eng. Asp. 404 (2012) 47.
[33] M. Almgren, V.M. Garamus, T. Asakawa and N. Jiang, J. Phy. Chem. B. 111 (2007) 7133.
[34] H. Belarbi, D. Bendedouch and F. Bouanani, J. Surfact. Deterg. 13 (2010) 433.
[35] D. Bendedouch, S. H. Chen, W. C. Koehler and J. S. Lin, J. Chem. Phy. 76 (1982) 5022.
[36] F. Bouanani, D. Bendedouch, C. Maitre, J. Teixeira and P. Hemery, Polym. Bull. 55 (2005) 429.
[37] P. Zheng, X. Zhang, J. Fang and W. Shen, J. Chem. Eng. Data, 61 (2016) 979.
[38] F. Bouanani, D. Bendedouch, P. Hemery and B. Bounaceur, Coll. Surf. A: Physicochem. Eng. Asp. 317 (2008) 751.
[39] H. Otmani, F. Bouanani and D. Bendedouch, Tenside. Surfact. Deterg. 56 (2019) 61.
[40] K. Szymczyk, J. Coll. Interf. Sci. 363 (2011) 223.
[41] M. Kotlarchyk, S.H. Chen, J. Chem. Phy. 79 (1983) 2461.
[42] L. Van Hove, Phy. Rev. 95 (1954) 249.
[43] J. Welch, V.A. Bloomfield, J. Polym. Sci. Polym. Phy. 11 (1973) 1855.
[44] P. Debye, J. Phy. Chem. 51 (1947) 18.
[45] J.S Higgins, H.C Benoit, Polymers and Neutron Scattering, Clarendon, Oxford, 1994.
[46] O. Kratky, G. Porod, J. Coll. Sci. 4 (1949) 35.
[47] J. N Israelachvili, D. J. Mitchell, and B. W. Ninham, J. Chem. Soc. Faraday. Trans. II. 72 (1976) 1525.
[48] T.Chakraborty, S. Ghosh and S. P. Moulik, J. Phy. Chem. 109 (2005) 14813.
[49] C. Tanford, J. Phy. Chem. 78 (1974) 2469.
[50] T. H. V. Ngo, C. Damas, R. Naejus and R. Coudert, J. Fluorine. Chem. 131 (2010) 704.
[51] H.Clint, J. Chem. Soc. Faraday. Trans. 71 (1975) 1327.
[52] D.N. Rubingh, in Solution Chemistry of Surfactants, K.L. Mittal, ed., Plenum Press, New York, 1979.
[53] J. Oremusová , Z. Vitková, A. Vitko, M. Tárník, E. Miklovičová, O. Ivánková, J. Murgaš and D. Krchňák, Molecules. 24 (2019) 651.
[54] S. S. Berr, J. Phys. Chem. 91 (1987) 4760.
[55] A. Guinier, G. Fournier, Small Angle Scattering of X-Rays, Wiley-Inter science, NewYork, 1955.
[56] E. J. Staples, G. Tiddy, J. Chem. Soc. Faraday. Trans. 74(1978) 2530.
[57] S. Ristori, C. Maggiulli, J. Appell, G. Marchionni, G. Martini, J. Phy. Chem. B. 101 (1997) 4155.
[58] M. Yang, J. Hao and H. Li, RSC Adv. 4 (2014) 40595.